Structural Monitoring and Maintenance, *Vol. 12, No. 3 (2025) 297-311*
https://doi.org/10.12989/smm.2025.12.3.297

Innovative foam-based laminated composite panels with embedded SMA strip for low-impact shock absorption

Abolghassem Zabihollah*, Rajesh B. Vuddandam[a] and Elisha S. Acquah[b]

Department of Mechanical, Environmental, and Civil Engineering, Tarleton State University, Stephenville, USA

(*Received May 31, 2025, Revised July 18, 2025, Accepted August 6, 2025*)

Abstract. Sandwich structures with Carbon Fiber Reinforced Polymer (CFRP) skins are being utilized in construction applications where impact loading is a critical concern. Incorporating foam into the core layer is a promising strategy to enhance structural stability and integrity under impact conditions. However, the geometry, material properties, and assembly of the foam layer significantly affect the energy absorption capacity of such structures. In conventional foam-based sandwich structures, while the inclusion of foam reduces the risk of catastrophic failure under impact, it often results in partial permanent deformation. To address this limitation, this study introduces an innovative Foam-Based Sandwich Panel (FBSP) with laminated layers made of CFRP as the skins, and Shape Memory Alloy (SMA) strips, termed SMA-FBSP. The SMA-FBSP integrates high-density foam in the core for enhanced energy absorption and embeds SMA strips to enable shape recovery after the structure being deformed due to impact load. Low-velocity impact and repetitive impact testing were conducted to simulate real-world scenarios and evaluate the performance of the SMA-FBSP. A proof-of-concept prototype was fabricated, demonstrating the capacity of the structure in shape recovery under low-velocity impact loading. The presence of SMA strips enable the sandwich panel to regain its original shape for low strain. However, at high strain, (~10%), the SMA-FBSP regained approximately 80% upon releasing the applied load. The induced strain is measured by an array of surface bounded Fiber Bragg Grating (FBG) sensor. This advancement highlights the potential of SMA-FBSP in applications requiring both high impact resistance and structural recovery.

Keywords: damping; energy absorption; foam core; laminated composite; low-velocity impact; sandwich panel; shape memory alloy; shape recovery; vibration

1. Introduction

Sandwich structures have emerged as a top solution in modern construction, providing lightweight efficiency and robust performance (Palomba *et al.* 2022). This construction strategy leverages a core principle: combining two high-strength skins with a lightweight core to optimize structural behavior. This configuration significantly enhances bending and torsional stiffness (Zhu *et al*. 2024), resulting in superior load distribution and mitigating the risk of buckling and collapse

*Corresponding author, Professor, E-mail: azabihollah@tarleton.edu
[a]Ph.D., E-mail: vuddandam@tarleton.edu
[b]Student, E-mail: elishasam.acquah@go.tarleton.edu

Copyright © 2025 Techno-Press, Ltd.
http://www.techno-press.org/?journal=smm&subpage=7 ISSN: 2288-6605 (Print), 2288-6613 (Online)

under stress (Kiakojouri *et al.* 2022). Beyond structural integrity, sandwich structures exhibit energy efficiency. The core material, strategically selected for its thermal properties (Song *et al.* 2024), provides exceptional insulation. Furthermore, these structures demonstrate remarkable resilience against impact loads due to the incorporation of energy-absorbing core materials (Tarlochan 2021). The changeability of sandwich structures extends across diverse sectors, including aerospace, automotive, marine, biomedical, robotics industries and building facades (Balasubramanian *et al*. 2021). Their lightweight nature, coupled with exceptional strength, simplifies handling and installation, enhancing overall project efficiency.

Over the past two decades, various techniques have been investigated to improve the impact performance of sandwich structures (Pol *et al.* 2012). Pol and Liaghat (2014) examined the influence of incorporating nanoparticles into the composite matrix on its dynamic behavior under high-velocity impacts. More recently, Astaraki *et al*. (2023) explored the effect of integrating shear thickening fluids into sandwich structures to enhance energy absorption under low-velocity impacts.

The integration of Shape Memory Alloys (SMAs) into foam-based sandwich panels (FBSP) represents a significant advancement in material technology, offering enhanced performance and durability (Zhao *et al.* 2025). Recent studies have demonstrated the effectiveness of integrating SMAs into foam-core sandwich panels to enhance impact resistance. Li *et al.* (2021) found that embedding SMA fibers in composite face-sheets reduced delamination area by 48.15% and increased load-bearing threshold by 32.75% under low-velocity impact. Another study observed that SMA wires prevented full perforation and reduced internal delamination in hybrid composite sandwich panels, with placement in the front face-sheet being most effective (Masoudi Moghaddam *et al.* 2020). Maher *et al*. (2022) extended this research to high-velocity impacts, showing that increasing the number of SMA wires and applying pre-strain significantly improved energy absorption in corrugated core composite sandwich panels. These studies collectively highlight the potential of SMA integration in enhancing the impact performance of sandwich panels. SMAs, embedded within the panel, undergo phase transformations in response to stress or temperature changes (Hahnlen 2012, Kim *et al*. 2002), effectively dissipating energy during impact events. This mechanism improves energy absorption, minimizing damage to the core and face sheets.

Furthermore, the inherent shape memory effect of SMAs allows the panel to recover its original form after an impact, reducing the risk of permanent deformation (Balasubramanian *et al*. 2021, Singh Rajput *et al*. 2022). In another study (Zabihollah *et al.* 2024), SMA wires were integrated into a 3D-printed beam to provide adaptive functionality, where the SMA wires were activated through an electric current to recover beam deflection. Besides sandwich panels, SMA has found its way in a variety of structural problems in civil engineering. SMAs have shown promise for enhancing the resilience and performance of bridge systems and concrete structures (Alshannag *et al.* 2023, Muntasir Billah *et al*. 2022). SMAs offer advantages such as high strength, superior fatigue resistance, and damping capacity, making them suitable for prestressing concrete beams and seismic strengthening of structures (Alshannag *et al*. 2023). Zabihollah *et al*. (2024) presents a novel approach for monitoring and controlling crack propagation in concrete beams using Fiber Bragg Grating (FBG) sensors and SMA wires.

The combination of SMAs with a foam core significantly enhances the overall structural integrity (Mostafa 2019, Samali *et al*. 2019, Sun *et al*. 2023, Thomas *et al.* 2025). SMAs contribute to the panel's tensile strength, improving its performance under bending loads and mitigating localized failures (Khalili *et al*. 2020). Additionally, SMAs exhibit favorable damping

properties (Huang *et al.* 2024), reducing vibrations and oscillations within the structure (Costanza *et al*. 2024). This improves overall system damping, contributing to occupant comfort and minimizing wear on structural components. By enhancing energy absorption, reducing permanent deformation, and improving damping capabilities, the integration of SMAs into foam-based sandwich structures extends their operational lifespan, leading to reduced maintenance costs and improved safety in structures subjected to harsh environmental conditions or dynamic loads. Recent developments in fabrication techniques, including 3D printing, may further expand the potential applications of SMAs in civil engineering field (Singh Rajput *et al*. 2022). However, challenges remain, including high manufacturing costs and limited knowledge transfer from research to practice (Alshannag *et al*. 2023).

The present work investigates the effectiveness of integration of SMA strip within a foam-core sandwich panel with laminated layers made of CFRP as skins in shape recovery and vibration control under external stimuli particularly low-velocity impact. To encounter the huge variation in material and mechanical properties through the thickness (layer of CFRP, foam, and SMA), a modified layerwise displacement theory has been used for modeling the SMA-FBSPs. The following section provides a brief review of the layerwise displacement theory used in the analysis of laminated structures, as well as the stress-strain behavior of SMA materials. To demonstrate the functionality and effectiveness of SMAs in shape recovery and damping control, an experimental setup was developed. Multiple specimens, each integrated with different types of foam, were fabricated and tested under low rate loading conditions.

2. Theoretical background

The proposed foam-based sandwich panel composed of laminated com CFRP skins embedded with SMA strips (SMA-FBSP). It is noted that there is a huge difference between the material properties at each layer of the skin as well as at the core, requiring a displacement theory that accounts for such material inhomogeneity through thickness. Layerwise displacement theory addresses this issue by considering individual displacement function at each layer. This section briefly describes the superiority of layerwise displacement theory in modeling laminated composite structures, particularly the SMA-FBSP.

2.1 Modeling of sandwich beams using layerwise displacement theory

Fig. 1 shows the schematic of a FBSP composed of three sections, namely laminated composite face layers on top and bottom, and a foam section in the middle.

According to layerwise displacement theory, the displacement of SMA-FBSP is defined as

$$u(x,z,t) = \sum_{r=1}^{N} u_r(x,t)\varphi_r(z),\ w(x,z,t) = \sum_{r=1}^{N} w_r(x,t)\varphi_r(z) \tag{1}$$

$$\varphi_r(z) = [1-\zeta \quad \zeta]\ , \quad \zeta = \frac{z}{h} \tag{2}$$

where the variables *u*, *w*, *h*, and *N* are the displacement along the length, *x*, through the thickness, *z*, the thickness of each layer/section, and the total number of layers through the thickness/section defined at each longitudinal node, respectively. The interpolation functions $\varphi_r(x)$ are defined between any two adjacent layers. For thin plate or when material in relatively homognious at the layer, a liniear fucntion (Eq. (2)) is considered as the interpolation fucntion. Furthuremore, that for thin laminate, displacements in

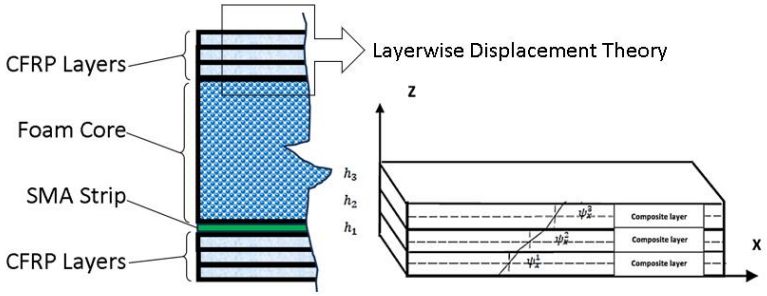

Fig. 1 Schematic layers of foam-based sandwich beam (FBSP)

z-direction between layers are negligible, $w(x,z,t) = w(x,t)$. One may realize that computation of element matrices for the SMA-FBSP using layerwise displacement theory requires computing Eq. (1) for each longitudinal node.

It is noted that foam and SMA materials can be considered as any number of layers through the thickness. However, considering that the material property of the foam and SMA are relatively constant through the thickness, they can be considered as one layer, thus having only two nodes through the thickness of such layers.

$$u_r(x,t) = \sum_{i=1}^{n} u_r^i(x,t)\emptyset_i(x),\ w_r(x,t) = \sum_{i=1}^{n} w_r^i(x,t)\emptyset_i(x) \tag{3}$$

where *n* is the number of nodes and $\phi_i(x)$ are the interpolation functions along the length, respectively. Using nodal displacement provided in Eq. (1) and proceeding with a conventional finite element approach, the matrix equation of motion for the SMA-FBSP is defined as (Momeni and Zabihollah 2025)

$$[M]\{\ddot{d}\} + [D]\{\dot{d}\} + [K]\{d\} = \{f(t)\} \tag{4}$$

where [*M*], [*K*], and [*D*] indicate the mass, stiffness, and structural damping matrices, respectively. It is noted that the structural damping matrix is a function of stiffness and mass matrices, $[D] = \alpha[K] + \beta[M]$. Vectors $\{d\}$ and $\{f(t)\}$ represent the nodal displacement and external force. It is noted that the force vector is determined according to the applied loading conditions.

2.2 Modeling of shape memory alloy

Most common SMAs exhibit two main effects, namely shape memory effect (SME) and superelasticity effect (SE). The shape memory effect (SME) is a characteristic of certain shape memory alloys (SMAs), such as Nitinol (a combination of nickel and titanium), where large deformations can be fully recovered through the application of heat, which induces a phase transformation. This property is primarily utilized in applications that require active control strategies, such as in the aerospace industry. In contrast, the superelasticity (SE) effect is more commonly employed in passive control applications, including civil infrastructure and building systems (e.g., bracings, beam- column joint, column buckling, etc.). The typical stress-strain behavior of Nitinol is illustrated in Fig. 2.

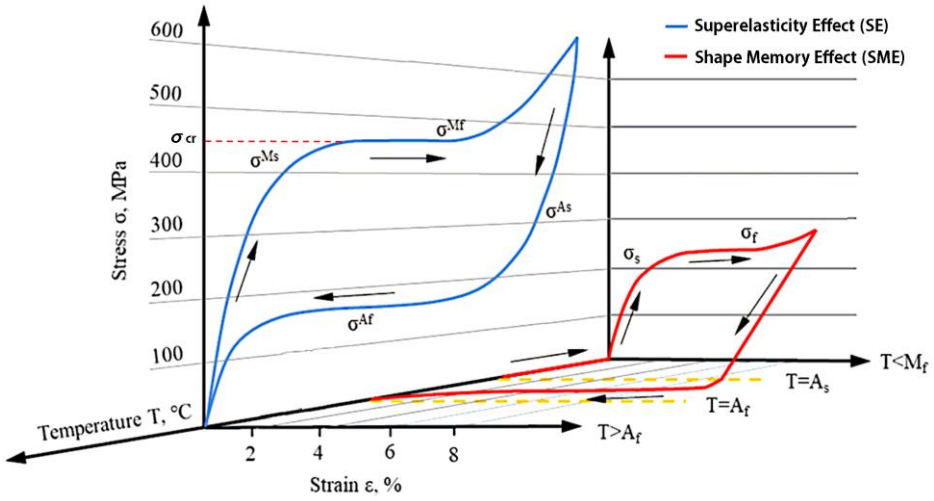

Fig. 2 Schematic diagram of thermomechanical behavior of a SMA wire/strip – Nitinol. Adapted from (Qiang *et al*. 2022). *M* and *A* denote the martensite and austenite phases, respectively, while the subscripts *s* and *f* indicate the start and finish of the phase transformation

Since the present work focuses on construction materials primarily used in buildings and civil applications, the following section provides a brief overview of the superelasticity (SE) concept only.

The superelasticity effect of SMA is a phenomenon where the material undergoes large recoverable strains (~ 8-10%) when subjected to mechanical loading and unloading. This phenomenon occurs when the operating temperature, during loading and unloading, is above or equal to the corresponding austenite start temperature (As) of the SMA.

It is noted that a full phase transformation occurs when the temperature is above the austenitic finish temperature. The stress-strain behavior of SMAs at SE condition is given by (Leo 2007)

$$\sigma(\varepsilon) = [E_A + \zeta(E_M - E_A)](\varepsilon - \varepsilon^T) \tag{5}$$

where σ, ε, and ε^T denote stress, the induced strain, and the phase transformation strain, respectively. E_A and E_M indicate Young's modulus of Austenite and Martensite phases, respectively. The term ζ is the phase transformation volume fraction which is zero in the fully austenite phase and one in the fully martensite phase. It is noted that at low strain, when the SMA is in the fully austenitic phase, it behaves like a conventional elastic material, i.e., $\sigma(\varepsilon) = EA\varepsilon$.

2.3 Impulse analysis of foam-based sandwich beam

Impulse loading is a very common type of load to which laminated sandwich beams are often subjected. An impact load is a load which is applied during a short period of time (Δt).

To determine the response of the SMA-FBSP, on the right side of dynamic Eq. (4), the force vector is considered as

$$F = \int_t^{t+\Delta t} f\,dt \tag{6}$$

Table 1 Thickness and volume fraction ratio of skin and core of the specimen

Specimen *	Thickness of skin – t_s (mm)	Thickness of core - t_c (mm)	Ratio of Volume Fraction Skin : Core : SMA (%)
CFRP-NH	2.54	6.35	44.45 : 55.56 : 0.00
CFRP-DH80	2.54	12.70	28.57 : 71.43 : 0.00
CFRP-HCCR	2.54	25.4	16.67 : 83.33 : 0.00
CFRP-NH-SMA	2.54	6.35	44.27 : 55.34 : 0.39
CFRP-DH80-SMA	2.54	12.7	28.50 : 71.25 : 0.25
CFRP-HCCR-SMA	2.54	25.4	16.64 : 83.21 : 0.15

* CFRP – Prepreg Carbon Fiber Reinforced Polymer (4 layer - 0/90/0/90); NH – Nomex Honeycomb core; DH80 – Divinycell H80 core; HCCR – High density Closed Cell Rubber core

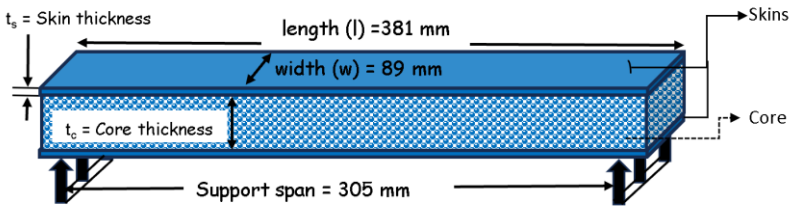

Fig. 3 Dimensions of the SMA-FBSP specimens

3. Materials and methods

This section thoroughly describes the experimental methodology used in this study, focusing on the SMA-FBSP specimens and the testing procedure. It includes detailed information on the materials used, the specimen preparation, and the testing setup.

The SMA-FBSP was fabricated as a proof-of-concept prototype to validate its performance through experimental testing, including low-velocity impact test, which were conducted to simulate real-world scenarios and evaluate the panel's response.

3.1 Material properties and specimen preparation

To investigate the effect of foam core layer on the dynamic behavior of SMA-FBSP, three common types of foam material have been selected. Table 1 provides the nomenclature, thickness of the skin and foam core, as well as their corresponding percentage volume fraction used for the specimen of SMA-FBSP.

Material property of CFRP: E =80 GPa, ρ = 1750 kg/m^3; SMA strip (1 mm × 4 mm × 381 mm), ρ = 6450 kg/m^3, the modulus elasticity at austenite (E_A) and martensite (E_M) are E_A = 84 GPa, E_M = 52.5 GPa, and austenite finish temperature is A_f = -10^{o}C. For industrial and practical applications, austenite finish temperature is sometimes refers to phase transition temperature. Fig. 3 shows the prototype of the SMA-FBSP specimen length, width and span used for three point bending test. Fig. 3 shows the schematic and dimensions of the specimen used for three-point bending. Fig. 4 shows the actual prototype of the SMA-FBSP specimens.

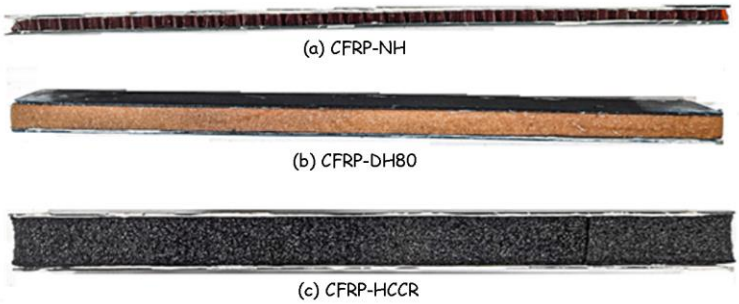

Fig. 4 SMA-FBSP specimens used in experimental testing

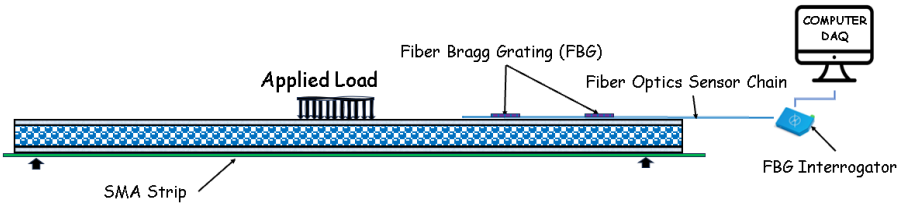

Fig. 5 Schematic of test setup for Superelasticity Effect (SE)

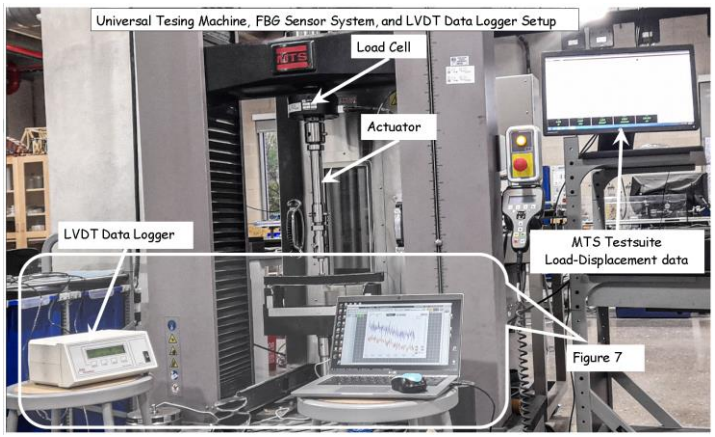

Fig. 6 UTM, FBG & LVDT test setup for CFRP-HCCR specimen without SMA

3.2 Three point bending test

To demonstrate the effect of SMA strip in shape recovery of the structure, a three-point test set up is developed. Fig. 5 provides a schematic representation of the three-point bending test setup, layout of test setup for superelasticity effect. The layout captures the positioning of Fiber Bragg Grating (FBG) sensors affixed to the specimens. The three-point bending test was conducted using a 22 kN capacity MTS Universal Testing Machine (UTM).

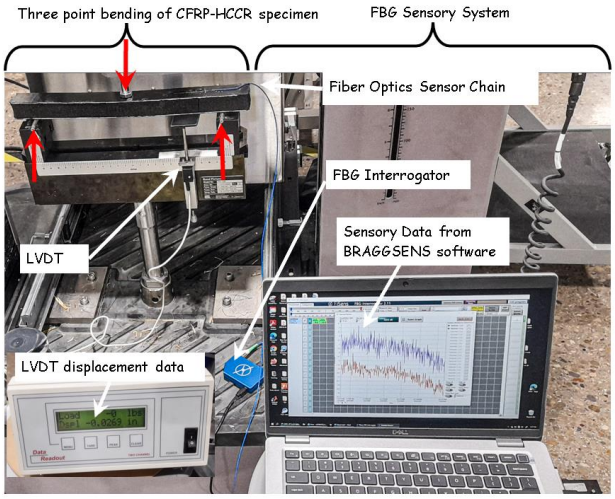

Fig. 7 Three-point bending of CFRP-HCCR specimen with SMA

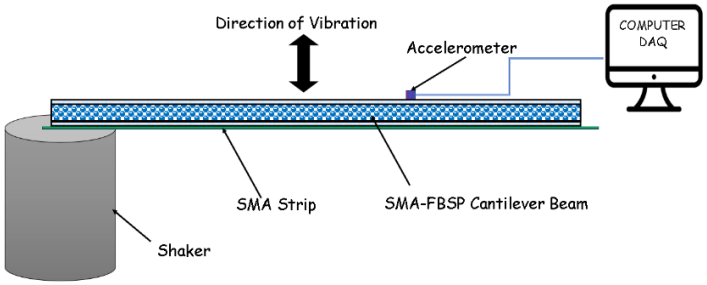

Fig. 8 Schematic of test setup to determine vibration response of SMA-FBSP

An FBG sensor array was attached to the top surface of the specimen, as shown in Figs. 5 and 6, to measure strain at two selected points along its length. To measure the deflection at selected point, an LVDT was placed at the quarter-point from the right support connected to a Datalogger to measure deflection along the specimen's length, as illustrated in Fig. 7.

The experimental investigation has been conducted for a CFRP-HCCR integrated with a strip of SMA mounted at the top face of the specimen. It is noted that in practical applications, the SMA strip should be secured within the beam at desired location through the thickness to provide the desired actuation function. İt is worth noting that adding SMA strip displaces the location of neutral axis of the beam and thus its performance under the load is altered.

3.3 Vibration testing

The schematic diagram provided in Fig. 8 shows the procedure of vibration testing. The actual setup for vibration testing is shown on Fig. 9. It is important to note that, in the experimental setup, the SMA strip was attached to the outer surface for simplicity and to ensure test repeatability. However, in practical applications, it can be positioned on the inner side of the top or bottom skins.

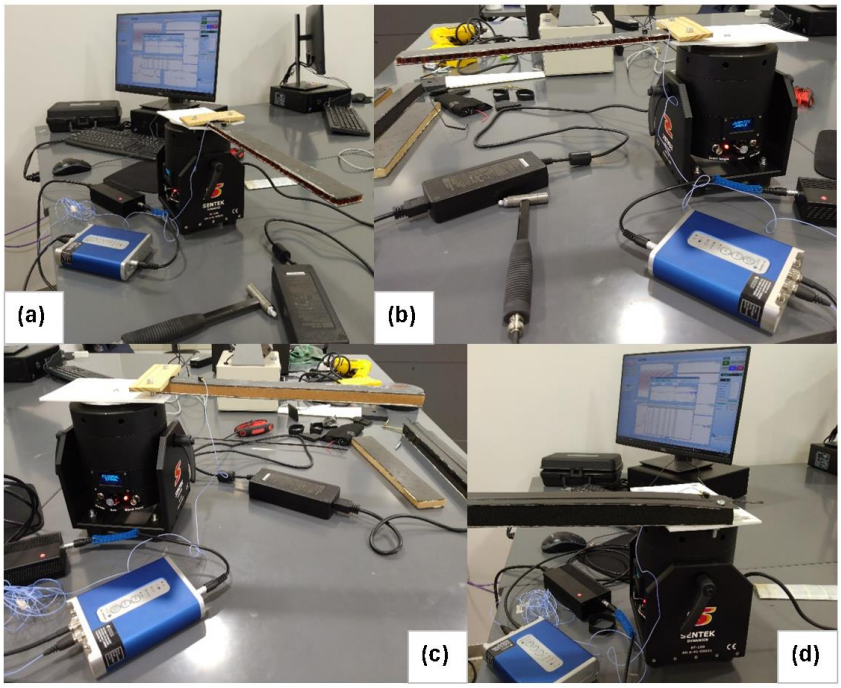

Fig. 9 Actual set up for Vibration test; (a), (b) CFRP-NH, (c) CFRP-DH80 and (d) CFRP-HCCR

4. Results and discussions

The following subsection describes the results obtained from the bending and dynamic tests.

4.1 Results of three-point bending test

Three-point bending test was conducted using the set up presented in Fig. 7. The load was applied under displacement control, with the actuator moving at a rate of 0.05 mm/s. Data was acquired at a frequency of 10 Hz. MTS TestSuite was used to generate the load vs. displacement graph, as shown in Fig. 10. To investigate the effect of SMA on load-displacement of foam-based sandwich beams, a sample FBSP with and without SMA is subjected to three-point bending test. Considering that SMA strip provides a similar trend of load-displacement behavior, only the result of one sample, namely, CFRP-HCCR has been presented in Fig. 10, in which CFRP-HCCR-SMA refers to the sample with surface bounded SMA.

The load-displacement response of the FBSP beam without the bonded SMA strip exhibits a relatively linear trend, with a constant slope of approximately 12° and a maximum load capacity of around 20 N. When a bonded SMA strip is added to the FBSP beam, the maximum load capacity significantly increases to approximately 70 N. However, the load-displacement behavior no longer follows the original linear pattern. Instead, the addition of the SMA alters the structural response, causing it to resemble the characteristic stress-strain behavior of the SMA material, as illustrated in Fig. 3.

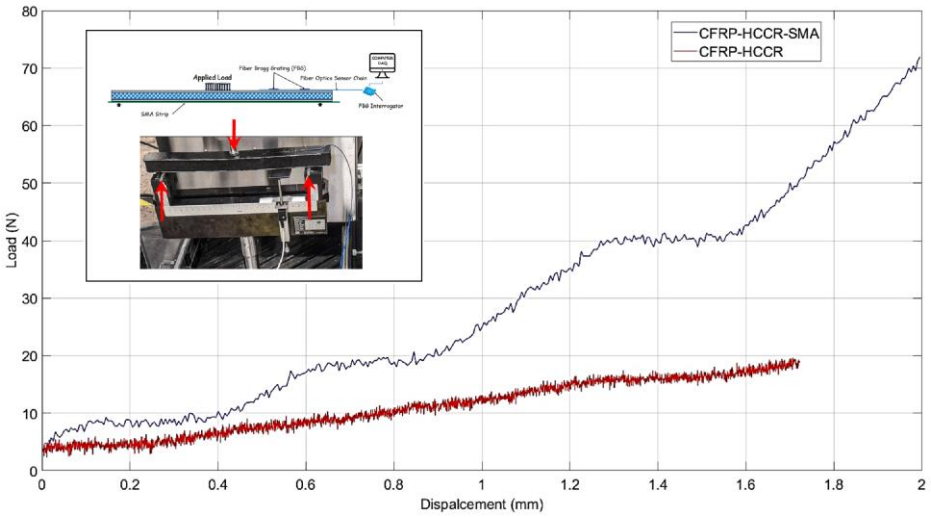

Fig. 10 Results of bending test; CFRP-HCCR with and without SMA

Notably, after reaching a critical load of about 40 N, the response enters a plateau region before increasing again.

4.2 Repeated low-speed implact testing

Three-point bending test was conducted using the set up presented in Fig. 7. The strain data was collected using an FBG interrogator, and the sensor output was recorded using BRAGGSENSE software, as shown in Fig. 11. For details of using FBG sensors for stain measurement, one may consult to (Zabihollah *et al*. 2024). To demonstrate the performance and functionality of the SMA-FBSP in shape recovery, various loading conditions were applied, including different peak loads and loading durations. The results show that the structural element with the SMA strip effectively recovers its deflection under repeated loading conditions.

It's important to note that the SMA's ability to recover shape can be significantly affected by cyclic loading conditions. However, for applications in buildings or civil structures, periodic loads typically result from accidental impacts or low-speed cyclic loading. Consequently, embedding an SMA strip in these structures could effectively address a wide range of loading scenarios, ensuring the recovery of their shape.

The capability of superelasticity of SMA strip in shape recovery of FBSP beam after removing the load has been studied by adding FBG sensors at the top layer of the beam as shown in Fig. 11. It is observed that the application of load deforms the beam to a high amount of strain. Upon removing the load, because of superelasticity of SMA, the deformation is released almost completely.

4.3 Modal analysis of SMA-FBSP

The natural frequency of SMA-FBSP beams for clamped-free boundary condition has been calculated using Eq. (4) for $f(t) = 0$. As the SMA material is homogeneous, then for the sake of

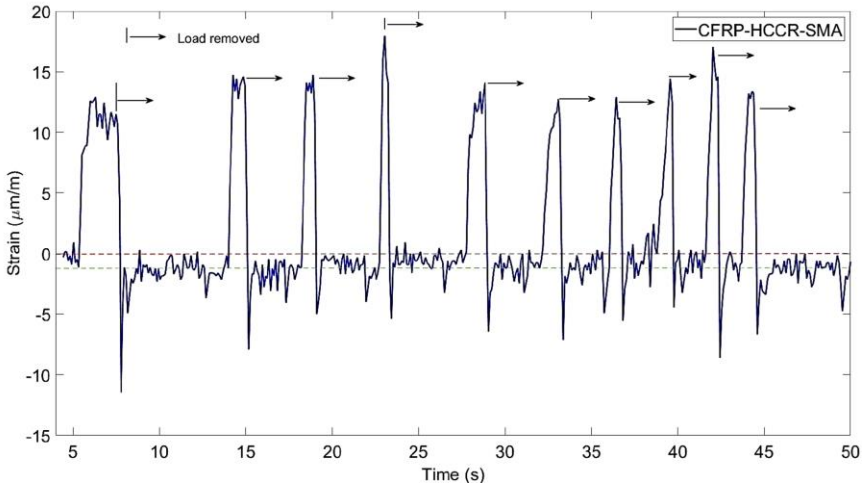

Fig. 11 Results of repeating bending test

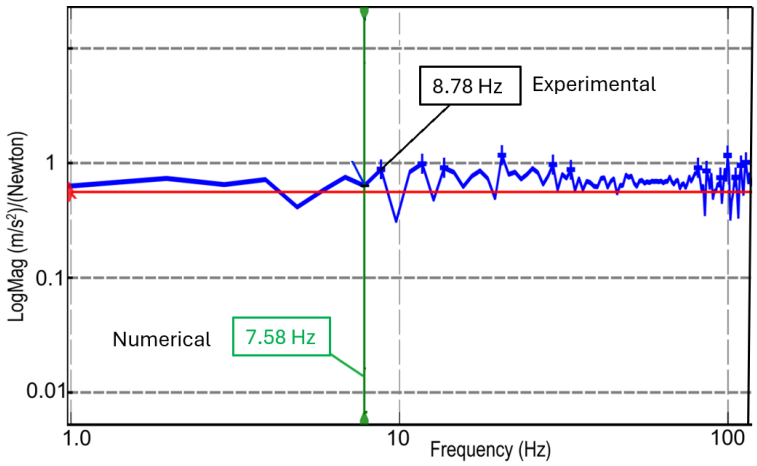

Fig. 12 Frequency response function of CFRP-NH-SMA

Table 2 Natural frequencies of sandwich beams for clamped-free boundary condition

Specimen	Natural Frequencies		
	Mode 1	Mode 2	Mode 3
CFRP-NH- SMA	7.58	49.34	141.33
CFRP-DH80-SMA	5.76	39.19	113.54
CFRP-HCCR-SMA	4.23	29.17	83.62

simplicity and reducing the computation, the SMA strip is considered as one layer with limited width. Table 2 provides the first three natural frequencies of SMA-FBSP beams.

Table 3 Experimental measurement of fundamental frequencies of sandwich beams for clamped-free boundary condition

	Specimen		
	CFRP-NH-SMA	CFRP-DH80	CFRP-HCCR
Fundamental Frequency (Hz)	8.78	5.86	4.23

Table 4 Experimental measurement of damping coefficients of sandwich beams for clamped-free boundary condition

	Specimen		
	CFRP-NH	CFRP-DH80	CFRP-HCCR
Damping Coefficient of Fundamental Mode	0.12547	0.17814	0.2592

As expected, the natural frequencies of the CFRP-NH-SMA are the highest, followed by CFRP-DH80-SMA and CFRP-HCCR-SMA. This is because the modulus of elasticity of NH material is higher than that of DH80 and HCCR. Higher elasticity results in higher stiffness and in turns, results in higher natural frequencies

4.4 Expermental vibration test

Vibration response of SMA-FBSP beams has been experimentally determined using the set up presented in Fig. 9. Fig. 12 provides the results obtained from CFRP-HCCR-SMA using the analysis software.

For the sake of brevity, the measurements for natural frequencies are extracted from the software and summarized in Table 3.

The values provided in boxes are given as markers for numerical values determined by solving Eq. (3) using MATLAB and experimental measurement. It is realized that the experimental measurement is higher than the numerical values. It is due to non-homogeneity in materials and assembly procedure that make the specimen stiffer than the modelling.

Table 4 provides experimental measurement of damping coefficients of different SMA-FBSP beams. It is noted that experimental setup may be used to determine the damping coefficients for higher modes. However, for applications on sandwich beam in buildings, higher modes are mainly of low priority.

As expected, model CFRP-HCCR-SMA damps faster than CFRP-DH80-SMA and CFRP-NH. This is due to the softer and thicker foam at the core layer. Furthermore, model CFRP-DH80 shows higher damping than that of CFRP-NH-SMA although the thickness of foam layer in CFRP-DH80 is higher than the thickness of core layer in CFRP-NH-SMA. This is expected when one realizes that the core layer in model CFRP-NH-SMA is composed of honeycomb structure with solid walls while the core layer of model CFRP-DH80-SMA is hard foam.

4.5 Impulse Loading

The impulse responses of three different SMA-FBSP beams have been determined by implementing Eq. (6) in Eq. (4) and solving the matrix in MATLAB. Fig. 13 illustrates the vibration response of the sandwich beams under impulse loading.

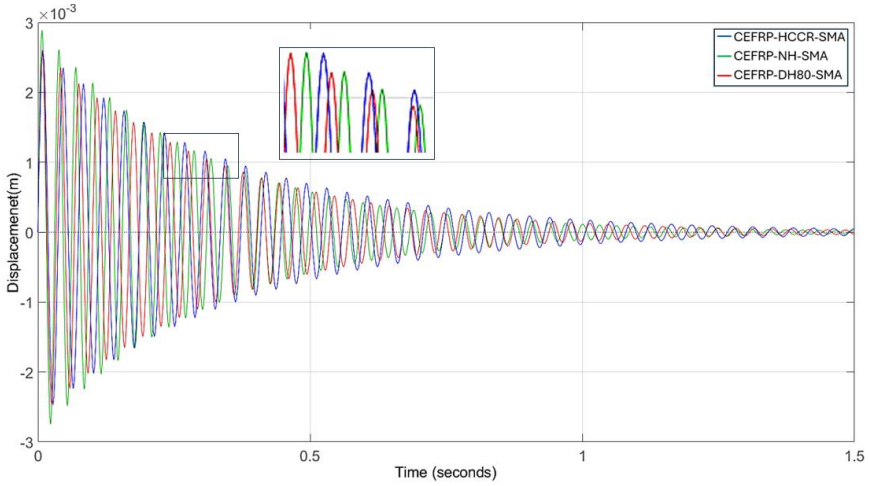

Fig. 13 Numerical time response determined using layerwise theory for different SMA-FBSP beams subjected to impulse loading

As observed, the CFRP-HCCR-SMA model suppresses vibrations more quickly than the other models. This is attributed to the higher damping coefficient of the softer foam. Consequently, the settling time for the CFRP-HCCR-SMA is approximately ten percent shorter than that of the CFRP-NH-SMA beam.

5. Conclusions

The influence of incorporating SMA strip in shape recovery of sandwich beams with laminated carbon fiber at the skins and foam materials at the core layer has been investigated. A modified layerwise displacement theory has been implemented to account for the variable materials properties of layers through the thickness of the beam. The specimens are subjected to three-point bending test till displacement beyond elastic limit. A Fiber Bragg Grating (FBG) sensor array is used to measure the strain.

It is realized that specimens with embedded SMA strips will recover up to 80% of displacement upon removing the applied load. The results show that by adding less than 0.4% volume fraction of SMA can recover up to 80% of the displacement when subjected to strains beyond elastic range.

In another test, the effect of SMA layer on dynamic response of the sandwich beam has been investigated. The effects of SMA as well as foam materials on the natural frequencies and damping coefficient of the specimens have been determined experimentally. The present work has potential use in designing sandwich panels for civil infrastructures susceptible to accidental impacts.

Acknowledgments

The authors wish to acknowledge the support provided by the Mayfield College of Engineering and the Departments of Mechanical, Environmental, and Civil Engineering at Tarleton State

University, USA. We sincerely appreciate Dr. Saman Momeni's valuable technical guidance and support, which significantly contributed to this work.

References

Alshannag, M.J., Alqarni, A.S. and Higazey, M.M. (2023), "Superelastic nickel–titanium (NiTi)-based smart alloys for enhancing the performance of concrete structures", *Materials*, **16**(12), 4333. https://doi.org/10.3390/ma16124333.

Astaraki, S., Zamani, E., Pol, M.H. and Hasannezhad, H. (2023), "Investigating the energy absorption properties of sandwich panels filled with shear thickening fluid with a weight fraction of 35% under low-velocity impact", *J. Compos. Mater.*, **58**(3), 361-375. https://doi:10.1177/00219983231225452.

Balasubramanian, M., Srimath, R., Vignesh, L. and Rajesh, S. (2021), "Application of shape memory alloys in engineering – A review", *J. Phys. Conference Series*, **2054**(1), 012078. https://doi.org/10.1088/1742-6596/2054/1/012078.

Costanza, G., Mercuri, S., Porroni, I. and Tata, M.E. (2024), "Shape memory alloys for self-centering seismic applications: A review on recent advancements", *Machines*, **12**(9), 628. https://doi.org/10.3390/machines12090628.

Hahnlen, R. (2012), "Characterization and modeling of active metal-matrix composites with embedded shape memory alloys", Ph.D. Dissertation, The Ohio State University, Columbus, OH, USA.

Huang, Y., Zhang, H., Fan, Q., Huang, Q., Shao, L., Zhan, X. and Wang, J. (2024), "The stiffness and damping characteristics of a rubber-based SMA composite shock absorber with a hyper-elastic SMA-constitutive model considering the loading rate", *Materials*, **17**(16), 4076. https://doi.org/10.3390/ma17164076.

Khalili, S., Khalili, S.M.R., Farsani, R.E. and Mahajan, P. (2020), "Flexural properties of sandwich composite panels with glass laminate aluminum reinforced epoxy face sheets sstrengthened by SMA wires", *Polymer Test.*, **89**, 106641. https://doi.org/10.1016/j.polymertesting.2020.106641.

Kiakojouri, F., De Biagi, V., Chiaia, B. and Sheidaii, M.R. (2022), "Strengthening and retrofitting techniques to mitigate progressive collapse: A critical review and future research agenda", *Eng. Struct.*, **262**, 114274. https://doi.org/10.1016/j.engstruct.2022.114274.

Kim, C., Park, B.-S. and Goo, N.-S. (2002), "Shape changes by coupled bending and twisting of shape-memory-alloy-embedded composite beams", *Smart Materials and Structures*, **11**(4), 519-526. https://doi.org/10.1088/0964-1726/11/4/306.

Leo, D. (2007), *Engineering Analysis of Smart Material Systems*, Wiley, Hoboken, NJ, USA.

Li, H., Jiang, C., Wu, Y., Huang, Y., Wan, Y. and Chen, R. (2021), "Experimental study on the low-velocity impact failure mechanism of foam core sandwich panels with shape memory alloy hybrid face-sheets", *Sci. Eng. Compos. Mater.*, **28**(1), 592-604. https://doi.org/10.1515/secm-2021-0059.

Maher, R., Khalili, S.M.R. and Eslami-Farsani, R. (2022), "Experimental analysis of corrugated core sandwich panel with smart composite face-sheets under high-velocity impact", *J. Compos. Mater.*, **56**(10), 1495-1511. https://doi.org/10.1177/00219983221077152.

Masoudi Moghaddam, S.A., Yarmohammad Tooski, M., Jabbari, M. and Khorshidvand, A.R. (2020), "Experimental investigation of sandwich panels with hybrid composite face sheets and embedded shape memory alloy wires under low velocity impact", *Polymer Compos.*, **41**(11), 4811-4829. https://doi.org/10.1002/pc.25754.

Momeni, S. and Zabihollah, A. (2025), "Effect of core material on random vibration behavior of foam-based laminated sandwich panels using a modified layerwise theory", *Mater. Res. Express*, **12**(1), 015701. https://doi.org/10.1088/2053-1591/ada2e2.

Mostafa, A. (2019), "Experimental and numerical investigation on enhancing the structural integrity of composite sandwich structure", *Adv. Struct. Eng.*, **22**(9), 2149-2162. https://doi.org/10.1177/1369433219836177.

Muntasir Billah, A., Rahman, J. and Zhang, Q. (2022), "Shape memory alloys (SMAs) for resilient bridges: A state-of-the-art review", *Structures*, **37**, 514-527. https://doi.org/10.1016/j.istruc.2022.01.034.

Palomba, G., Epasto, G. and Crupi, V. (2022), "Lightweight sandwich structures for marine applications: A review", *Mech. Adv. Mater. Struct.*, **29**(26), 4839-4864. https://doi.org/10.1080/15376494.2021.1941448.

Pol, M.H. and Liaghat, G.H. (2016), "Investigation of the high velocity impact behavior of nanocomposites", *Polymer Compos.*, **37(**4), 1173-1179. https://doi.org/10.1002/pc.23281.

Pol, M.H., Liaghat, G. and Hajiarazi, F. (2012), "Effect of nanoclay on ballistic behavior of woven fabric composites: Experimental investigation", *J. Compos. Mater.*, **47**(13), 1563-1573. https://doi:10.1177/0021998312449768.

Qiang, X., Chen, L. and Jiang, X. (2022), "Achievements and perspectives on Fe-based shape memory alloys for rehabilitation of reinforced concrete bridges: An overview", *Materials*, **15**(22), 8089. https://doi.org/10.3390/ma15228089.

Samali, B., Nemati, S., Sharafi, P., Tahmoorian, F. and Sanati, F. (2019), "Structural performance of polyurethane foam-filled building composite panels: A state-of-the-art", *J. Compos. Sci.*, **3**(2), 40. https://doi.org/10.3390/jcs3020040.

Singh Rajput, G., Vora, J., Prajapati, P. and Chaudhari, R. (2022), "Areas of recent developments for shape memory alloy: A review", *Mater. Today: Proceedings*, **62**, 7194-7198. https://doi.org/10.1016/j.matpr.2022.03.407.

Song, Z., Su, L., Yuan, M., Shang, S. and Cui, S. (2024), "Self-cleaning, energy-saving aerogel composites possessed sandwich structure: Improving indoor comfort with excellent thermal insulation and acoustic performance", *Energ. Buildings*, **310**, 114098. https://doi.org/10.1016/j.enbuild.2024.114098.

Sun, C., Albustani, H., Phadnis, V.A., Saleh, M.N., Cantwell, W.J. and Guan, Z. (2023), "Improving the structural integrity of foam-core sandwich composites using continuous carbon fiber stitching", *Compos. Struct.*, **324**, 117509. https://doi.org/10.1016/j.compstruct.2023.117509.

Tarlochan, F. (2021), "Sandwich structures for energy absorption applications: A review", *Materials*, **14**(16), 4731. https://doi.org/10.3390/ma14164731.

Thomas, K.K., Hassan, N.M., Bahroun, Z. and Awad, M. (2025), "Exploring the role of shape memory alloys in advanced composite sandwich panels and laminates", *Compos. Part C: Open Access*, **16**, 100557. https://doi.org/10.1016/j.jcomc.2025.100557.

Zabihollah, A., Vuddandam, R., Bardowell, S. and Does, B. (2024), "Shape control of an adaptive 3D-printed beam with integrated FBG sensors and SMA wires: Modeling and experimental testing", *ISSS J. Micro Smart Syst.*, **13**(2), 47-57. https://doi.org/10.1007/s41683-024-00126-6.

Zabihollah, A., Vuddandam, R. and Sandoval, R. (2024), "Monitoring and control of crack propagation of flexural SMA-fiber reinforced concrete members", *Active and Passive Smart Structures and Integrated Systems XVIII*, **12946**, 360-369. https://doi.org/10.1117/12.3010057.

Zabihollah, A., Hajyalikhani, P. and Vuddandam, R. (2024), "Evaluation of embedded FBG sensors for strain monitoring of residential timber buildings under various wind speeds", *Struct. Monit. Maint.*, **11**(4), 263-275. https://doi.org/10.12989/smm.2024.11.4.263.

Zhao, W., Zeng, C., Liu, L., Leng, J. and Liu, Y. (2025), "Shape memory sandwich structure with reprogrammable shape and mechanical properties", *Compos. Struct.*, **351**, 118604. https://doi.org/10.1016/j.compstruct.2024.118604.

Zhu, Y., Polyzos, E. and Pyl, L. (2024), "Stiffness optimization of sandwich structures with elastically isotropic lattice core", *Thin Wall. Struct.*, **195**, 111408. https://doi.org/10.1016/j.tws.2023.111408.